

Comparative study of the effects of electron irradiation and natural disorder in single crystals of $\text{SrFe}_2(\text{As}_{1-x}\text{P}_x)_2$ superconductor ($x = 0.35$)

C. P. Strehlow, M. Konczykowski, J. A. Murphy, S. Teknowijoyo, K. Cho, M. A. Tanatar, T. Kobayashi, S. Miyasaka, S. Tajima, R. Prozorov

► To cite this version:

C. P. Strehlow, M. Konczykowski, J. A. Murphy, S. Teknowijoyo, K. Cho, et al.. Comparative study of the effects of electron irradiation and natural disorder in single crystals of $\text{SrFe}_2(\text{As}_{1-x}\text{P}_x)_2$ superconductor ($x = 0.35$). *Physical Review B: Condensed matter and materials physics*, American Physical Society, 2014, 90, pp.5. <10.1103/PhysRevB.90.020508>. <hal-01074701>

HAL Id: hal-01074701

<https://hal-polytechnique.archives-ouvertes.fr/hal-01074701>

Submitted on 12 Dec 2014

HAL is a multi-disciplinary open access archive for the deposit and dissemination of scientific research documents, whether they are published or not. The documents may come from teaching and research institutions in France or abroad, or from public or private research centers.

L'archive ouverte pluridisciplinaire **HAL**, est destinée au dépôt et à la diffusion de documents scientifiques de niveau recherche, publiés ou non, émanant des établissements d'enseignement et de recherche français ou étrangers, des laboratoires publics ou privés.

Comparative study of the effects of electron irradiation and natural disorder in single crystals of $\text{SrFe}_2(\text{As}_{1-x}\text{P}_x)_2$ superconductor ($x = 0.35$)

C. P. Strehlow,¹ M. Kończykowski,² J. A. Murphy,¹ S. Teknowijoyo,¹ K. Cho,¹ M. A. Tanatar,¹ T. Kobayashi,³ S. Miyasaka,^{3,4} S. Tajima,^{3,4} and R. Prozorov^{1,*}

¹The Ames Laboratory and Department of Physics & Astronomy, Iowa State University, Ames, Iowa 50011, USA

²Laboratoire des Solides Irradiés, CNRS-UMR 7642 & CEA-DSM-IRAMIS, Ecole Polytechnique, F-91128 Palaiseau Cedex, France

³Department of Physics, Graduate School of Science, Osaka University, Toyonaka, Osaka 560-0043, Japan

⁴JST, Transformative Research-Project on Iron-Pnictides (TRIP), Chiyoda, Tokyo 102-0075, Japan

(Received 27 May 2014; revised manuscript received 30 June 2014; published 28 July 2014)

The London penetration depth $\lambda(T)$ was measured in single crystals of a $\text{SrFe}_2(\text{As}_{1-x}\text{P}_x)_2$ ($x = 0.35$) iron-based superconductor. The influence of disorder on the transition temperature T_c and on $\lambda(T)$ was investigated. The effects of scattering controlled by the annealing of as-grown crystals was compared with the effects of artificial disorder introduced by 2.5 MeV electron irradiation. The low-temperature behavior of $\lambda(T)$ can be described by a power-law function $\Delta\lambda(T) = AT^n$, with the exponent n close to one in pristine annealed samples, as expected for a superconducting gap with line nodes. Upon electron irradiation with a dose of $1.2 \times 10^{19} \text{ e/cm}^2$, the exponent n increases rapidly, exceeding a dirty limit value of $n = 2$, implying that the nodes in the superconducting gap are accidental and can be lifted by the disorder. The variation of the exponent n with T_c is much stronger in the irradiated crystals compared to the crystals in which disorder was controlled by the annealing of the growth defects. We discuss the results in terms of different influence of different types of disorder on intraband and interband scattering.

DOI: 10.1103/PhysRevB.90.020508

PACS number(s): 74.70.Xa, 74.20.Rp, 74.62.Dh

The pairing mechanism in Fe-based superconductors has been the focal point of many theoretical and experimental works [1,2]. The proximity to magnetism and high superconducting transition temperatures T_c in the upper 50 K range prompted the search for a nonphonon mechanism of superconductivity [3]. Based on early experiments, Mazin *et al.* [3,4] suggested an unconventional superconducting state with interband pairing in which the superconducting gap function changes sign between different sheets of the Fermi surface, but remains full (without line nodes) on each sheet. Experimental verification of this so-called s_{\pm} pairing mechanism quickly became a main point of superconducting gap structure studies in iron-based materials.

The verification of the k -space sign-changing gap in iron-based superconductors turned out to be more difficult than it was in the cuprates, in which sign change along a single Fermi surface was proven by directional phase sensitive experiments [5,6]. It was suggested that impurity scattering can be used as a probe of a sign-changing gap [7]. This approach becomes significantly more powerful when, in addition to the suppression of T_c , other thermodynamic quantities, such as the London penetration depth, are studied on the same samples [8,9]. At low temperatures, the temperature dependence of the superconducting gap becomes negligible and the total variation is determined by the temperature-induced population of quasiparticles. In the clean limit, $\Delta\lambda(T)$ is exponentially attenuated in a full gap superconductor (including multiband s_{++} , such as MgB_2 [10]), but has a T -linear behavior in superconductors with line nodes [8,11]. In the dirty limit, $\lambda(T)$ in conventional s and s_{++} superconductors remains exponential, but evolves into a T^2 dependence in both line-nodal and

nodeless s_{\pm} cases [8,11]. However, in the s_{\pm} superconductor with accidental nodes, this convergence is nonmonotonic. First, the nodes are lifted and the behavior becomes close to exponential. Upon a further increase of scattering, more additional in-gap states are created and a gapless T^2 dirty limit is eventually reached [8,12]. In nodeless s_{\pm} this limit is reached from the exponential behavior [13,14]. A convenient way to describe all possible scenarios of low-temperature evolution of the penetration depth is to use the power-law function $\Delta\lambda(T) = AT^n$. Exponential behavior is seen as large values of the exponent n . However, if the nodes are symmetry imposed, as in d -wave materials, the exponent grows monotonically from $n = 1$ to $n = 2$ and never exceeds this terminal value.

Artificial disorder in superconductors can be introduced in a controlled way by irradiation. Depending on the irradiation type and energy, the induced defects have different characteristics. Early studies of T_c [9,15,16] and $\lambda(T)$ in $\text{Ba}(\text{Fe}_{1-x}\text{Co}_x)_2\text{As}_2$ (BaCo122) [9] and $\text{Ba}(\text{Fe}_{1-x}\text{Ni}_x)_2\text{As}_2$ (BaNi122) [9,16] used heavy ion irradiation that produces one-dimensional columnar defects [15]. The analysis of T_c and of the exponent n of the power-law function used to fit the temperature-dependent London penetration depth $\Delta\lambda = AT^n$ was consistent with the predictions of the s_{\pm} model. A later study in the optimally hole-doped $(\text{Ba}_{1-x}\text{K}_x)\text{Fe}_2\text{As}_2$ ($x = 0.4$) [17] found a crossover of $\Delta\lambda(T)$ from exponential to a T^2 at very high irradiation doses, but virtually no change in T_c , most probably indicating a dominant intraband pairing interaction in this compound [8]. Irradiation with 2 MeV α particles [18] and 3 MeV protons [19–21], both creating clusterlike defects [22], found a much faster suppression of T_c than in the case of columnar defects, but still much slower than originally predicted for a simplified “symmetric” s_{\pm} scenario [23]. More recently, the predictions for the s_{\pm} scenario were significantly relaxed in a realistic “asymmetric” model [8]. These calculations were used to fit a significant variation of T_c

*Corresponding author: prozorov@ameslab.gov

induced by 2.5 MeV electron irradiation in BaRu122 [24]. A similar suppression rate was found in other 122 compounds, including BaCo122 and Ba(AsP)122 [25]. In the material of this study, $\text{SrFe}_2(\text{As}_{1-x}\text{P}_x)_2$, the effect of postgrowth disorder was studied previously by measuring both T_c and $\lambda(T)$ in samples before and after annealing [26]. It was known that annealing of optimally ($x = 0.35$) substituted samples leads to an enhancement of T_c typically from 25 to 27 K to almost 35 K [27,28]. The analysis of the low-temperature behavior of the penetration depth was unambiguously consistent with the presence of line nodes in the gap [26], very similar to another material with isovalent P substitution, $\text{BaFe}_2(\text{As}_{1-x}\text{P}_x)_2$ [29].

In this Rapid Communication we report a comparative study of the effects of artificial and natural disorder on T_c and the quasiparticle excitations in single crystals of $\text{SrFe}_2(\text{As}_{1-x}\text{P}_x)_2$ with an optimal level of isovalent phosphorus substitution, $x = 0.35$. The natural defects include screw dislocations and related residual after-growth strain and other faults in the crystal structure. These defects are typically extended in one or two dimensions. The electrons, on the other hand, introduce a pointlike disorder. Our main observation is that electron irradiation and natural defects change T_c and the London penetration depth $\lambda(T)$ in significantly distinct ways. We relate this dissimilarity to a possible difference in the scattering amplitude and characteristic spatial range of the scattering potential.

Single crystals of $\text{SrFe}_2(\text{As}_{1-x}\text{P}_x)_2$ with an optimal isovalent substitution level, $x = 0.35$, were grown from stoichiometric mixtures of Sr, FeAs, and FeP powders. Details of the growth and postgrowth annealing are described elsewhere [27,28]. The samples studied were from two different batches, A and B. They were cleaved with a razor blade from the inner parts of larger single crystals and had two shiny cleavage surfaces, and thicknesses of about 60–70 μm . The side surfaces of the samples were also cleaved along the a axes in the plane, and the samples were close to $0.6 \times 0.6 \text{ mm}^2$ in the surface area. Prior to the penetration depth measurements, the same samples were measured using a magneto-optical technique [30] to check for possible cracks and macroscopic inhomogeneity. We found a typical Bean profile of the magnetic induction distribution with no visible anomalies, reflecting the high sample quality and good magnetic uniformity.

Measurements of the in-plane London penetration depth were performed by using a self-resonating tunnel diode resonator (TDR), which is essentially a radio-frequency (14 MHz) magnetic susceptibility measurement [31,32]. In the experiment, the sample was mounted at the end of a high-purity sapphire rod whose temperature can be precisely controlled. The rod with the sample was inserted into a coil of the tank circuit with an excitation ac magnetic field of $H_{ac} \approx 20 \text{ mOe}$. As the sample was cooled through the superconducting transition, the changes of the sample magnetic susceptibility $\chi(T)$ changed the inductance of the coil and led to a shift of $\Delta f(T)$ in the characteristic resonant frequency of the LC oscillator. The susceptibility $\chi(T)$ is related to $\Delta f(T)$ via $\Delta f(T) = -G4\pi\chi(T)$, where G is a geometric calibration factor, $G = f_0 V_s / 2V_c(1 - N)$, N is the demagnetization factor, V_s is the sample volume, and V_c is the coil volume [32]. The calibration factor G was determined by physically pulling the sample out of the inductor coil at

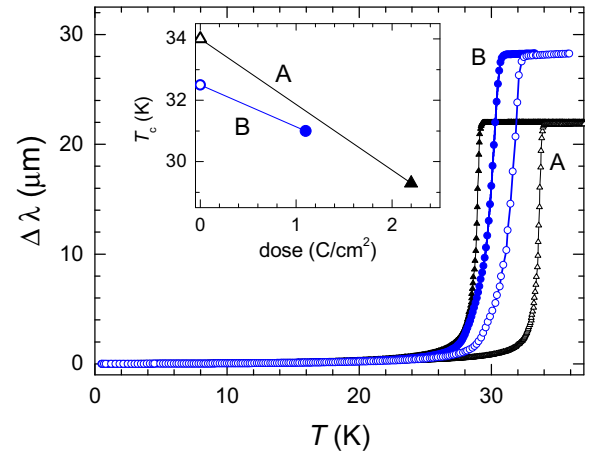


FIG. 1. (Color online) Full temperature range variation of the London penetration depth, $\Delta\lambda(T)$, in two single crystals of $\text{SrFe}_2(\text{As}_{1-x}\text{P}_x)_2$, $x = 0.35$, A (black triangles) and B (blue circles) before (open symbols) and after (solid symbols) irradiation with doses of 2.2 and 1.1 C/cm^2 , respectively. The superconducting transition temperature T_c was defined as the peak in the temperature-dependent derivative of the signal $d\lambda/dT$, roughly corresponding to the midpoint of the transition. The inset shows the change of T_c as a function of the irradiation dose.

the lowest temperature and measuring the full frequency shift. The magnetic susceptibility can be written in terms of the London penetration depth λ and the characteristic sample dimension R , $4\pi\chi = (\lambda/R)\tanh(R/\lambda) - 1$, from which λ may be extracted [31,32]. The 2.5 MeV electron irradiation was performed at the SIRIUS Pelletron linear accelerator operated by the Laboratoire des Solides Irradiés (LSI) at the Ecole Polytechnique in Palaiseau, France. The irradiation dose is represented here in C/cm^2 . To convert to electrons per cm^2 , this number needs to be divided by the electron charge e . The sample of batch A was exposed to a dose of 2.2 C/cm^2 and the sample of batch B was exposed to 1.1 C/cm^2 . After the irradiation, the samples were warmed up to room temperature, which results in up to 30% partial annealing of the defects [24]. Importantly, the comparative measurements of the effect of irradiation were conducted on physically the same samples before and after treatment.

Figure 1 shows the variation of the London penetration depth in samples A and B over the whole temperature range from the base temperature of 0.5 K to above T_c . Open and solid symbols show the data for the same samples before and after irradiation. The inset in Fig. 1 shows that the two studied samples exhibit a similar slope of T_c versus the irradiation dose. Also, both samples show sharp superconducting transitions before and after the irradiation, suggesting a spatially homogeneous distribution of the induced defects. This is not strange considering that the electrons at an energy of 2.5 MeV have a stoppage distance of more than 500 μm , which is significantly longer than sample thickness.

Figure 2 zooms at the low-temperature, up to $T_c/3$, variation of the London penetration depth $\Delta\lambda(T)$ in pristine and irradiated samples A and B the data for two samples are plotted versus the reduced temperature T/T_c (left panel) and versus $(T/T_c)^2$ (right panel). The data for

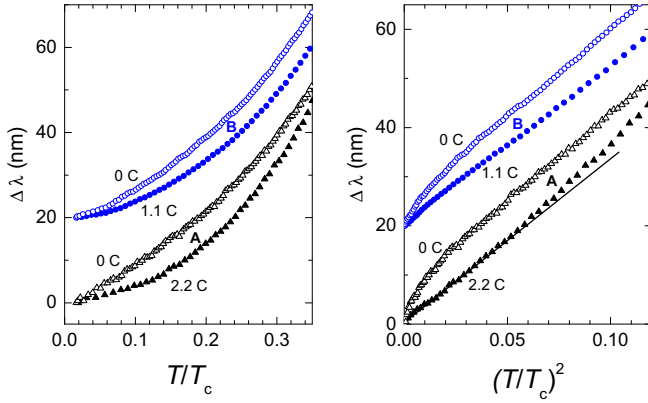


FIG. 2. (Color online) Low-temperature variation of the London penetration depth in single crystals of $\text{SrFe}_2(\text{As}_{1-x}\text{P}_x)_2$, $x = 0.35$, plotted vs reduced temperature T/T_c (left panel) and vs $(T/T_c)^2$ (right panel). The data for sample A in the pristine annealed state are shown by open black triangles, and after the irradiation with 2.2 C/cm^2 by solid black triangles. The data for sample B before (blue open circles) and after 1.1 C/cm^2 irradiation (blue solid circles) are offset by 20 nm to avoid overlapping. The line in the right panel is a guide to the eye to show a slight upward curvature suggesting $n > 2$ after electron irradiation with 2.2 C/cm^2 .

the pristine state (before irradiation) are in agreement with the results of our previous study (see Fig. 3 below [26]). The electron irradiation significantly decreases the total variation of $\Delta\lambda(T)$ reflected in an increased exponent n . In sample B irradiated with 1.1 C/cm^2 , the exponent $n = 1.8$. In sample A, exposed to 2.2 C/cm^2 electron irradiation, we find $n = 2.26$. Plotting the data versus $(T/T_c)^2$ clearly shows that the sample

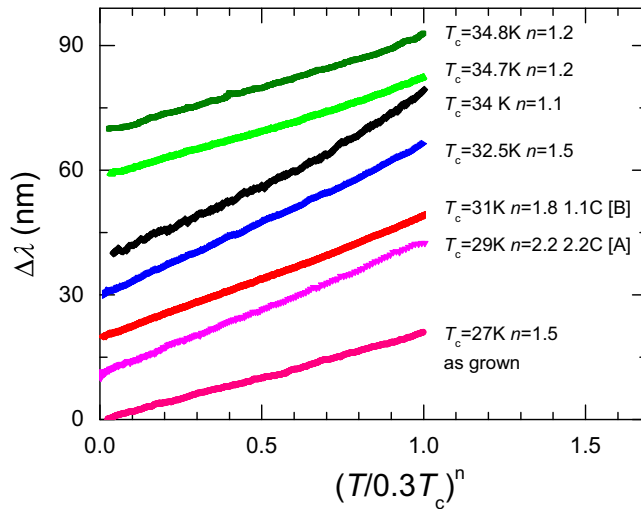


FIG. 3. (Color online) $\Delta\lambda(T)$ vs $(T/0.3T_c)^n$, with n as a fitting parameter selected to linearize the data. The data for pristine annealed samples (top four curves, $T_c \geq 32.5 \text{ K}$) are well described with a single power law each over the whole range. The data for samples with growth defects show $n = 1.5$, while the samples subjected to electron irradiation show a rapid increase of n with T_c suppression. Note that for all samples $\Delta\lambda(0.3T_c)$ is about the same.

with a larger dose reveals an upward curvature, suggesting that $n > 2$ at low temperatures.

It is generally accepted that the exponent $n > 2$ cannot be explained by the effect of disorder in superconductors with symmetry-imposed line nodes. There is, however, a caveat, that in a multiband superconductor the range over which a characteristic T^2 dependence is observed can be significantly smaller than in a single gap superconductor. To study this possibility, in Fig. 3 we performed a different analysis of the functional form of $\Delta\lambda(T)$. Here $\Delta\lambda(T)$ for each sample was plotted versus $(T/0.3T_c)^n$, where n was chosen to produce the closest to linear dependence. Previously, we showed that the data for both as-grown low T_c samples and annealed high T_c samples can be well described by using the Hirschfeld-Goldenfeld interpolation formula [11,26], with the effective temperature T^* increasing with the amount of disorder. The data for these samples can be actually linearized using an exponent n close to 1, for all samples with $T_c > 34 \text{ K}$, clearly suggesting line nodes in the superconducting gap. The exponent n increases for samples with lower T_c . However, this linearization procedure does not produce nonmonotonic dependencies as expected for pronounced multigap effects. Therefore our data are best described by a true power law, with $n > 2$ in the most irradiated sample.

To summarize our findings, Fig. 4 shows the exponent n plotted versus T_c , controlled either by the growth defects or by the defects induced by electron irradiation. The data for the two types of disorder reveal a striking dissimilarity. While the variation of both n and T_c in the samples with growth disorder is consistent with an impurity effect in superconductors with symmetry-imposed line nodes, irradiation brings the exponent n above the range allowed for such superconductors, despite a significantly milder suppression of T_c . Furthermore, we do not observe any increase of $\Delta\lambda(T)$ on cooling [33], which could be suggestive of paramagnetic effects induced by the irradiation, so the difference between the effects is unlikely to be nonmagnetic versus magnetic scattering. The irradiation with electrons at energies between 1 and 10 MeV is known to

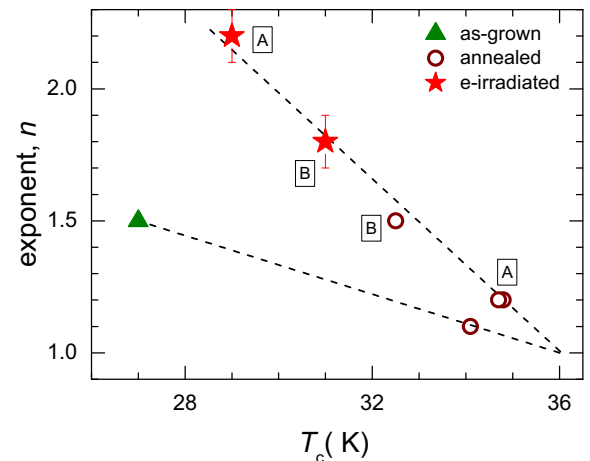


FIG. 4. (Color online) The exponent n of the power-law fit of $\Delta\lambda(T)$ from Fig. 3, vs T_c . Note the significantly smaller exponents for as-grown and annealed compared to the samples with irradiation defects. The dashed lines are guides for the eye.

create primarily Frenkel pairs of vacancies and interstitial ions [22]. Interstitials tend to migrate and disappear at surfaces and other sinks in the crystal structure, leaving vacancies as pointlike disorder [22]. On the other hand, disorder in as-grown samples mostly appears as dislocations, which have a long-range elastic strain field, and therefore these two types of defects have significantly different characteristics. It is therefore conceivable that scattering on these defects is characterized by a notably different momentum transfer. In other words, the strength and characteristic range and dimensionality of the scattering potentials corresponding to these defects are quite different.

In a generic s_{\pm} multiband scenario of superconductivity, applicable to iron pnictides, the interplay between intraband and interband pairing channels leads to a diverse phase diagram of the possible gap structures. A sign-changing gap is locked by the interband pairing, while the ratio between the interband to intraband pairing potentials determines gap amplitudes and anisotropies [1,2]. These considerations helped to explain the strong doping evolution of the superconducting gap observed experimentally in pnictides that were fully gapped at optimal doping [34,35]. Our present and previous studies show that the superconducting gap of $\text{SrFe}_2(\text{As}_{1-x}\text{P}_x)_2$ has line nodes [26,36,37], similar to $\text{BaFe}_2(\text{As}_{1-x}\text{P}_x)_2$ [29]. The nature of these nodes can be probed by studying the effect of a controlled disorder. Scattering in interband and intraband channels has a very different effect on superconductivity [1,2,8,38]. Scattering with a small momentum transfer would transfer the electrons only within the same Fermi surface sheets (intraband scattering), while scattering between different sheets of the Fermi surface necessitates a large momentum transfer. Since point defects have a characteristic size of a unit cell or less, the characteristic wave vector is of the order of $Q \sim 2\pi/a$, a sizable fraction of the Brillouin zone. For this type of disorder we would naturally expect a strong contribution to the interband scattering channel. By the same logic, extended defects would be characterized by a much smaller Q , and contribute mostly to the intraband scattering. This and previous studies show that $\text{SrFe}_2(\text{As}_{1-x}\text{P}_x)_2$ has a superconducting gap

with line nodes [26,36,37]. Small Q scattering within each sheet of the Fermi surface in this situation will be quite similar to the usual effect of disorder in nodal superconductors, as we observed here for the growth defects. Large Q scattering on point defects, however, will lift the nodes and drive the gap structure towards the full gap, if the nodes are accidental [8]. Our observation of $n > 2$ supports this scenario. An alternative scenario by Korshunov *et al.* suggests a transition from s_{\pm} to a conventional s_{++} state as a function of disorder [38].

In conclusion, we found dramatically different effects of artificial and natural disorder of as-grown samples on the superconducting transition temperature T_c and on quasiparticle excitations measured by a variation of the London penetration depth in isoelectron-substituted $\text{SrFe}_2(\text{As}_{1-x}\text{P}_x)_2$. The response to the postgrowth disorder is similar to the usual effect of disorder in nodal superconductors. The response to electron irradiation is notably different, suggesting the evolution of the superconducting gap structure from nodal to nodeless, which is expected for accidental nodes. We relate the difference between the two types of disorder to the difference in the characteristic scattering wave vector Q , with small Q for postgrowth disorder and large Q for a point-type disorder.

Note added. Recently a related work appeared where the authors studied the effects of electron irradiation on both T_c and penetration depth in another isovalent-substituted compound, $\text{BaFe}_2(\text{As}_{1-x}\text{P}_x)_2$ [12]. Their results support the accidental node scenario in this class of nodal iron pnictides.

The work in Ames was supported by the U.S. Department of Energy (DOE), Office of Science, Basic Energy Sciences, Materials Science and Engineering Division. Ames Laboratory is operated for the U.S. DOE by Iowa State University under Contract No. DE-AC02-07CH11358. We thank the SIRIUS team, B. Boizot, V. Metayer, and J. Losco, for running electron irradiation at Ecole Polytechnique (supported by EMIR network, proposal 11-11-0121.) Work at Osaka was partly supported by a Grant-in-Aid IRONSEA from the Japan Science and Technology Agency (JST).

-
- [1] A. V. Chubukov, *Annu. Rev. Condens. Matter Phys.* **3**, 57 (2012).
 [2] P. J. Hirschfeld, M. M. Korshunov, and I. I. Mazin, *Rep. Prog. Phys.* **74**, 124508 (2011)
 [3] I. I. Mazin, D. J. Singh, M. D. Johannes, and M. H. Du, *Phys. Rev. Lett.* **101**, 057003 (2008).
 [4] I. I. Mazin, *Nature (London)* **464**, 183 (2010).
 [5] C. C. Tsuei and J. R. Kirtley, *Rev. Mod. Phys.* **72**, 969 (2000).
 [6] D. J. van Harlingen, *Rev. Mod. Phys.* **67**, 515 (1995).
 [7] A. Glatz and A. E. Koshelev, *Phys. Rev. B* **82**, 012507 (2010).
 [8] Y. Wang, A. Kreisel, P. J. Hirschfeld, and V. Mishra, *Phys. Rev. B* **87**, 094504 (2013).
 [9] H. Kim, R. T. Gordon, M. A. Tanatar, J. Hua, U. Welp, W. K. Kwok, N. Ni, S. L. Bud'ko, P. C. Canfield, A. B. Vorontsov, and R. Prozorov, *Phys. Rev. B* **82**, 060518 (2010).
 [10] R. Prozorov, R. W. Giannetta, S. L. Bud'ko, and P. C. Canfield, *Phys. Rev. B* **64**, 180501 (2001).
 [11] P. J. Hirschfeld and N. Goldenfeld, *Phys. Rev. B* **48**, 4219 (1993).
 [12] Y. Mizukami, M. Konczykowski, Y. Kawamoto, S. Kurata, S. Kasahara, K. Hashimoto, V. Mishra, A. Kreisel, Y. Wang, P. J. Hirschfeld, Y. Matsuda, and T. Shibauchi, [arXiv:1405.6951](https://arxiv.org/abs/1405.6951).
 [13] K. Hashimoto, T. Shibauchi, S. Kasahara, K. Ikada, S. Tonegawa, T. Kato, R. Okazaki, C. J. van der Beek, M. Konczykowski, H. Takeya, K. Hirata, T. Terashima, and Y. Matsuda, *Phys. Rev. Lett.* **102**, 207001 (2009).
 [14] H. Kim, M. A. Tanatar, W. E. Straszheim, K. Cho, J. Murphy, N. Spyrisson, J.-Ph. Reid, B. Shen, H.-H. Wen, R. M. Fernandes, and R. Prozorov, [arXiv:1406.2369](https://arxiv.org/abs/1406.2369).
 [15] Y. Nakajima, Y. Tsuchiya, T. Taen, T. Tamegai, S. Okayasu, and M. Sasase, *Phys. Rev. B* **80**, 012510 (2009).
 [16] J. Murphy, M. A. Tanatar, Hyunsoo Kim, W. Kwok, U. Welp, D. Graf, J. S. Brooks, S. L. Budko, P. C. Canfield, and R. Prozorov, *Phys. Rev. B* **88**, 054514 (2013).

- [17] N. W. Salovich, Hyunsoo Kim, Ajay K. Ghosh, R. W. Giannetta, W. Kwok, U. Welp, B. Shen, S. Zhu, H.-H. Wen, M. A. Tanatar, and R. Prozorov, *Phys. Rev. B* **87**, 180502 (2013).
- [18] C. Tarantini, M. Putti, A. Gurevich, Y. Shen, R. K. Singh, J. M. Rowell, N. Newman, D. C. Larbalestier, P. Cheng, Y. Jia, and H.-H. Wen, *Phys. Rev. Lett.* **104**, 087002 (2010).
- [19] L. Fang, Y. Jia, J. A. Schlueter, A. Kayani, Z. L. Xiao, H. Claus, U. Welp, A. E. Koshelev, G. W. Crabtree, and W.-K. Kwok, *Phys. Rev. B* **84**, 140504 (2011).
- [20] Y. Nakajima, T. Taen, Y. Tsuchiya, T. Tamegai, H. Kitamura, and T. Murakami, *Phys. Rev. B* **82**, 220504 (2010).
- [21] T. Taen, F. Ohtake, H. Akiyama, H. Inoue, Y. Sun, S. Pyon, T. Tamegai, and H. Kitamura, *Phys. Rev. B* **88**, 224514 (2013).
- [22] A. C. Damask and G. J. Dienes, *Point Defects in Metals* (Gordon & Breach, London, 1963).
- [23] S. Onari and H. Kontani, *Phys. Rev. Lett.* **103**, 177001 (2009).
- [24] R. Prozorov, M. Konczykowski, M. A. Tanatar, A. Thaler, S. L. Bud'ko, P. C. Canfield, V. Mishra, and P. J. Hirschfeld, [arXiv:1405.3255](https://arxiv.org/abs/1405.3255).
- [25] C. J. van der Beek, S. Demirdis, D. Colson, F. Rullier-Albenque, Y. Fasano, T. Shibauchi, Y. Matsuda, S. Kasahara, P. Gierlowski, and M. Konczykowski, *J. Phys.: Conf. Ser.* **449**, 012023 (2013).
- [26] J. Murphy, C. P. Strehlow, K. Cho, M. A. Tanatar, N. Salovich, R. W. Giannetta, T. Kobayashi, S. Miyasaka, S. Tajima, and R. Prozorov, *Phys. Rev. B* **87**, 140505 (2013).
- [27] T. Kobayashi, S. Miyasaka, and S. Tajima, *J. Phys. Soc. Jpn.* **81**, SB045 (2012).
- [28] T. Kobayashi, S. Miyasaka, S. Tajima, T. Nakano, Y. Nozue, N. Chikumoto, H. Nakao, R. Kumai, and Y. Murakami, *Phys. Rev. B* **87**, 174520 (2013).
- [29] K. Hashimoto, K. Cho, T. Shibauchi, S. Kasahara, Y. Mizukami, R. Katsumata, Y. Tsuruhara, T. Terashima, H. Ikeda, M. A. Tanatar, H. Kitano, N. Salovich, R. W. Giannetta, P. Walmsley, A. Carrington, R. Prozorov, and Y. Matsuda, *Science* **336**, 1554 (2012).
- [30] R. Prozorov, M. A. Tanatar, B. Roy, N. Ni, S. L. Bud'ko, P. C. Canfield, J. Hua, U. Welp, and W. K. Kwok, *Phys. Rev. B* **81**, 094509 (2010).
- [31] R. Prozorov and R. W. Giannetta, *Supercond. Sci. Technol.* **19**, R41 (2006).
- [32] R. Prozorov, R. W. Giannetta, A. Carrington, and F. M. Araujo-Moreira, *Phys. Rev. B* **62**, 115 (2000).
- [33] C. Martin, M. E. Tillman, H. Kim, M. A. Tanatar, S. K. Kim, A. Kreyssig, R. T. Gordon, M. D. Vannette, S. Nandi, V. G. Kogan, S. L. Budko, P. C. Canfield, A. I. Goldman, and R. Prozorov, *Phys. Rev. Lett.* **102**, 247002 (2009).
- [34] M. A. Tanatar, J.-Ph. Reid, H. Shakeripour, X. G. Luo, N. Doiron-Leyraud, N. Ni, S. L. Bud'ko, P. C. Canfield, R. Prozorov, and L. Taillefer, *Phys. Rev. Lett.* **104**, 067002 (2010).
- [35] J.-Ph. Reid, M. A. Tanatar, X. G. Luo, H. Shakeripour, N. Doiron-Leyraud, N. Ni, S. L. Bud'ko, P. C. Canfield, R. Prozorov, and L. Taillefer, *Phys. Rev. B* **82**, 064501 (2010).
- [36] T. Dulguun, H. Mukuda, T. Kobayashi, F. Engetsu, H. Kinouchi, M. Yashima, Y. Kitaoka, S. Miyasaka, and S. Tajima, *Phys. Rev. B* **85**, 144515 (2012).
- [37] H. Takahashi, T. Okada, Y. Imai, K. Kitagawa, K. Matsubayashi, Y. Uwatoko, and A. Maeda, *Phys. Rev. B* **86**, 144525 (2012).
- [38] D. V. Efremov, M. M. Korshunov, O. V. Dolgov, A. A. Golubov, and P. J. Hirschfeld, *Phys. Rev. B* **84**, 180512 (2011).